High Energy Physics and Nuclear Physics

Volume 12, No. 1

Dependence of Interaction Cross Sections of High Energy Cosmic Ray Iron Nuclei (E ≥ 3.6A GeV) on Atomic Weight of Targets

Ren Guoxiao, Zhou Yinzao, and Huang Rongqing

(Institute of High Energy Physics, Academia Sinica, Beijing.)

Using plastic nuclear track detector CR-39 interleaved with various targets, nucleus-nucleus interaction cross sections of high energy Fe nuclei (E ≥3.6AGeV) with C, Al, Fe and Cu nuclei at balloon level in Beijing area were measured and the dependence of interaction cross sections on the atomic weight of targets was obtained.

---

1. INTRODUCTION

The nucleus-nucleus interaction cross section in high energy is one of the fundamental data of high energy nuclear physics and also the important data for the study of the origin and propagation of cosmic rays. So far, the energy of heavy ion accelerator has only reached 2AGeV[1], the measurement of the cross section of nucleus-nucleus interaction, especially heavy nucleus-nucleus interaction in high energy, still relys on cosmic ray experiment which, however, lacks systematic work. This situation is also true with the study of the target-mass dependence of interaction cross section of high energy heavy nuclei which may reflect some features of nuclear structure and collision process.

By the geomagnetic cut-off of the cosmic ray charged particles in Beijing area, the iron flux with energies higher than 3.6AGeV can be obtained. Using CR-39 plastic track detector to identify the charge of nuclei, we have measured the cross section of the iron nuclei interacting with four kinds of targets in two balloon flights.

Received on January 6, 1987

1) Recently, lighter nuclei, such as ^{16}O are accelerated to 200AGeV.

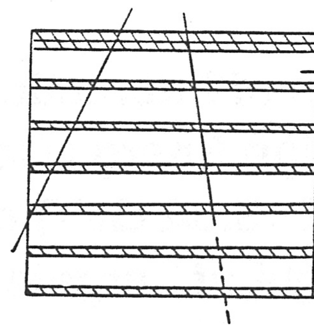

FIG. 1 Schematic diagram of detector structure.

2. EXPERIMENT

2.1 Detector

The detector structure of CR-39 sheets interleaved with target material is shown in Fig.1. In aluminium target, 6 layers of alumunium plates with a thickness of 1.8 cm each were used; in carbon target, 5 layers with a thickness of 0.83 cm each were used, and in iron and cooper ones, only 3 layers of target plates with a thickness of 1.23 cm and 1.21 cm were used respectively. The total amount of materials were 9.34, 29.16, 29.00 and 32.38 g/cm^2 for carbon, aluminium, iron and cooper respectively.

According to our previous analysis [1], when there is no large number of incident particles, the error of the mean free path (mfp) λ of the particles interacting with target mainly results from the statistical fluctuation of the number n of interactions. The standard deviation is

$$\sigma(\lambda) = \lambda/\sqrt{n}, \tag{1}$$

TABLE 1
Situation of two balloon flights

Launching Site: Xianhe balloon station; vertical geomagnetic cut off rigidity 9.8 GV		
Launching time	May 14, 1982	May 31, 1985
Detector type	CR-39 (pure)	CR-39 (DOP)
Detector area	544.5 cm^2 (Al target)	272.2 cm^2 (C target) 544.5 cm^2 (Cu, Fe target)
Exposure time	9.5 h	15.3 h
Average flight height	36.8 km	35.4 km
Average atmospheric depth	4.6 g/cm^2	5.8 g/cm^2

The error from the determination of interaction points is much smaller than $\sigma(\lambda)$ due to the thickness H of target layer and can be approximated as

$$\Delta\lambda = \frac{H}{n}\sqrt{\frac{N_0}{12}}, \tag{2}$$

where N_0 is the incident particle number. So we can choose an appropriate target thickness H to satisfy the condition

$$\Delta\lambda < \sigma(\lambda). \tag{3}$$

2.2 Exposure

The situation of the two balloon flights is shown in Table 1. The flight height is shown in Fig.2.

2.3 Etching and Measurement of CR-39

We etched the exposed CR-39 sheets after dividing them into several groups. The etching condition of each group was somewhat different in order to obtain good track quality for different type of CR-39. The etching solution used was 6.25–6.80N ± 0.1N NaOH with a temperature of 65–70°C ± 0.03°C. The etching lasted 30–40 hours.

After scanning the first two sheets of each detector and measuring the major axis (e) and minor axis (e') of the ellipse on the up and down surfaces of each penetrating particle, the etching rate V and particle-incident angle θ of each track were calculated by the following two formulas:

$$V = \sqrt{(1-\beta^2)^2 + 4\alpha^2}/(1-\beta^2), \tag{4}$$

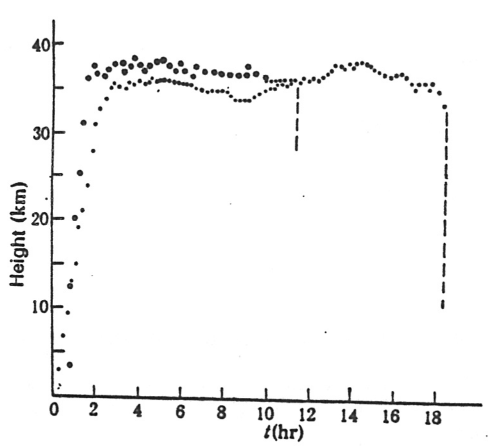

FIG. 2 Height vs. time of two balloon flights.

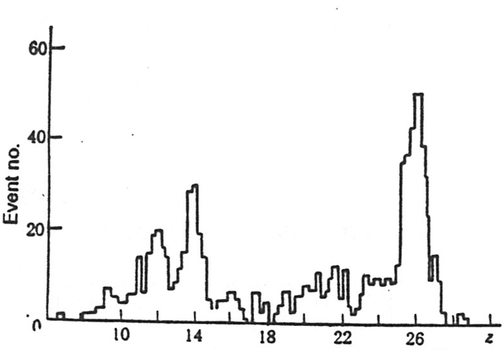

FIG. 3 Charge distribution of cosmic ray nuclei at balloon height (data were uncorrected according to the detecting efficiency).

$$\sin\theta = (1+\beta^2)/\sqrt{(1-\beta^2)^2+4\alpha^4}, \tag{5}$$

where $\alpha = e/2B$, $\beta = e'/2B$ and B is the etched thickness on the CR-39 surface.

After correcting the incident angles, the distribution of etching rate V was obtained and the iron nuclei was separated. The charge distribution of about 900 cosmic ray nuclei is shown in Fig.3. The charge resolution of the iron nuclei is 0.5–0.9e for different types of CR-39.

According to the tracing method described in Ref.[2] we can determine the interaction points having $\Delta Z \geq 1$ inside the detector and the layers with which the tracks escape from the detector without interaction. Then the path x_i of each iron nucleus in the detector was obtained.

2.4 Data Processing Method

The maximum likelihood estimator of nuclear interaction mean free path is [3]

$$\hat{\lambda} = \sum_{i=1}^{N_0} x_i/n. \tag{6}$$

Our further analysis shows that Eq.(6) is not an unbiased estimator. It can become one only when the path is calculated at the last (nth) particle interacting inside the target rather than at all particles(see Appendix).

3. RESULTS AND DISCUSSIONS

The data and results are listed in Table 2.

The square root of the cross section shows a good relation with the cubic root of the atomic weight of target A_T as shown in Fig.4. Fitted with data we have

$$\sigma^{1/2} = 0.202 + 0.405 A_T^{1/3}, \tag{7}$$

which is consistent with Bradt-Peters' cross section formula

$$\sigma = \pi r_0^2 (A_T^{1/3} + A_P^{1/3} - b)^2. \tag{8}$$

TABLE 2

Experimental data, and obtained mfp and corresponding cross section values

Target	Incident particle number N_0	Interacting particle number n	Sum of particle path (cm)	$\hat{\lambda}_{\Delta Z \geq 1}$ (cm)	Cross section $\sigma_{\Delta Z \geq 1}$ (b)
C	223	130	852.03	6.55 ± 0.57	1.35 ± 0.12
Al	322	205	1805.74	8.81 ± 0.62	1.88 ± 0.13
Fe	407	264	1031.55	3.91 ± 0.24	3.22 ± 0.18
Cu	453	323	1141.17	3.52 ± 0.20	3.35 ± 0.19

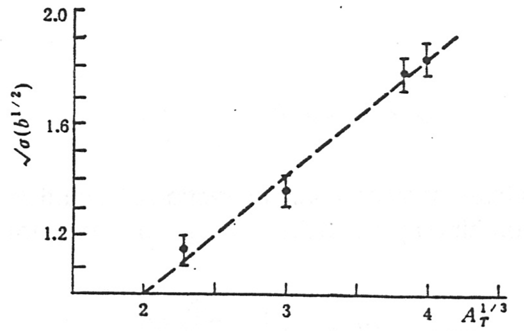

FIG. 4 $\sigma^{1/2}$ vs $A_T^{1/3}$

where A_p is the atomic weight of incident nucleus, r_0 is nucleon radii and b is overlapping constant. We have $r_0 = 2.28 \pm 0.09$ fm, $b = 3.22 \pm 1.15$ by fitting our data with Eq.(8).

Our result shows that the charge resolution of CR-39 we used is capable of determining the nuclear interaction with a charge change $\Delta Z \geq 1$. It also proves that a thicker target will not influence the precision of cross section determination in the case of low flux in cosmic ray experiment.

APPENDIX

Assume that the incident particles are perpendicular to the detector, for the convenience of calculation, D denotes the thickness of detector (see Fig.5). When N_0 particles are incident, the interacting particle number n within the detector obeys the truncated binomial distribution

$$P(n) = \frac{1}{1 - q^{N_0}} C_{N_0}^{n} p^n q^{N_0 - n}, \quad (n = 1, 2, \cdots, N_0) \qquad \text{(A-1)}$$

The path x_i of the interacting particle obeys the truncated exponential distribution

$$P(x_i) = \frac{1}{\lambda p} e^{-x_i/\lambda}, \quad (i = 1, 2, \cdots, n; \ 0 < x_i < D) \qquad \text{(A-2)}$$

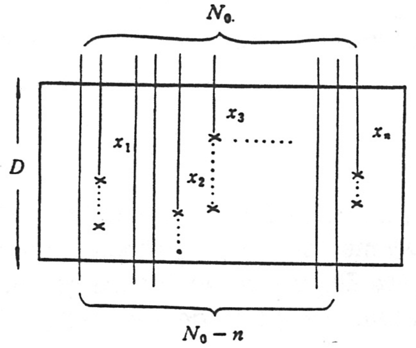

FIG. 5 Schematic diagram of particle interaction.

where

$$p = 1 - e^{-D/\lambda}, \quad q = 1 - p \tag{A-3}$$

are the probabilities of interaction and non-interaction of a particle inside the detector.

The normalized combined probability density function of random variables x_i and n is

$$P(x_i, n) = \frac{1}{1 - q^{N_0}} C_{N_0}^{n} q^{N_0 - n} \frac{1}{\lambda^n} e^{-\sum_1^n x_i/\lambda},$$

$$(n = 1, 2, \cdots, N_0; \ 0 < x_i < D). \tag{A-4}$$

which generates the expectation of the maximum likelihood estimator $\hat{\lambda}$

$$\langle \hat{\lambda} \rangle = \lambda - D/p + N_0 D \cdot \left\langle \frac{1}{n} \right\rangle, \tag{A-5}$$

where $\left\langle \frac{1}{n} \right\rangle = \sum_1^{N_0} \frac{1}{n} P(n)$. It can be seen that $<\hat{\lambda}>$ is not equal λ, but is related with N_0 and D. Therefore, from Eq.(6) $\hat{\lambda}$ is a biased estimator of mfp.

On the other hand, if we only calculate the particles before the n-th interacting one, then the incident particle number N_0 is a random variable which follows the distribution

$$P(N_0) = C_{N_0-1}^{n-1} p^n q^{N_0-n}, \quad (N_0 = n, n+1, \cdots). \tag{A-6}$$

The characteristic function of $\hat{\lambda}$ of Eq.(6) is obtained from the characteristic functions of x_i and N_0. It is as follows:

$$\varphi_{\hat{\lambda}}(t) = \left(1 - i\frac{\lambda}{n} t\right)^{-n}, \tag{A-7}$$

and so

$$\langle \hat{\lambda} \rangle = \frac{1}{i} \frac{d\varphi_{\hat{\lambda}}(t)}{dt}\bigg|_{t=0} = \lambda, \tag{A-8}$$

Now, the expectation of $\hat{\lambda}$ is exactly equal to λ, which shows that Eq.(6) is an unbiased estimator of mfp.

ACKNOWLEDGEMENT

Thanks to those who participated in our work. Chen Mingyuan took part in the work of aluminium target. All members of the balloon group of IHEP were responsible for the balloon launching. Ma Zhiguo assembled the gondola. Wang Genhua helped us to measure the temperature change inside the gondola during the flights and Zhu

Qingqi, Wu Mei and Li Tipei discussed with us over the statistical method. We would like to express our sincere thanks to all of them.

REFERENCES

[1] Ren Guoxiao et al., Annual Report of Cosmic Ray Laboratory, IHEP, Academia Sinica, (1983)94.
[2] Ren Guoxiao et al., High Energy Physics and Nuclear Physics, 8(1984), 664.
[3] Wu Mei et al., High Energy Physics and Nuclear Physics, 11(1987), 145.